# MSN: Multi-Style Network for Trajectory Prediction

Conghao Wong, Beihao Xia, Qinmu Peng, Wei Yuan, and Xinge You, Senior Member, IEEE

Abstract—Trajectory prediction aims at forecasting agents' possible future locations considering their observations along with the video context. It is strongly required by a lot of autonomous platforms like tracking, detection, robot navigation, self-driving cars, and many other computer vision applications. Whether it is agents' internal personality factors, interactive behaviors with the neighborhood, or the influence of surroundings, all of them might represent impacts on agents' future plannings. However, many previous methods model and predict agents' behaviors with the same strategy or the "single" feature distribution, making them challenging to give predictions with sufficient style differences. This manuscript proposes the Multi-Style Network (MSN), which utilizes style hypothesis and stylized prediction two sub-networks, to give agents multi-style predictions in a novel categorical way adaptively. We use agents' end-point plannings and their interaction context as the basis for the behavior classification, so as to adaptively learn multiple diverse behavior styles through a series of style channels in the network. Then, we assume one by one that the target agents will plan their future behaviors according to each of these categorized styles, thus utilizing different style channels to give a series of predictions with significant style differences in parallel. Experiments show that the proposed MSN outperforms current state-of-the-art methods up to 10% - 20% quantitatively on two widely used datasets, and presents better multi-style characteristics qualitatively.

Index Terms—Trajectory prediction, Multi-style, Hidden behavior category, Transformer.

## I. INTRODUCTION

nalyzing and understanding agents' activities or behaviors in images or videos are beneficial, crucial but challenging in the intelligent world. This study explores agents' behaviors through trajectory prediction, which is a novel and effective computer vision task. Trajectory prediction aims to forecast agents' potential future trajectories based on their historical positions, surroundings, and possible interactive behaviors. Due to trajectories' ease of acquisition and simplicity of analysis, the application of trajectory prediction has become more and more widespread. Its analyzed results and forecasted trajectories could be used as one of the primary input to a lot of intelligent vision systems and platforms, such as object detection [1], [2], object tracking [3], [4], robotic navigation [5], autonomous driving [6]–[9], behavior analysis [10]–[12], and many other computer vision applications. However, whether it is the interaction between heterogeneous agents, the inhomogeneous physical environment, or agents' uncertain intention and diverse behavior styles, all these factors will bring enormous challenges within the prediction process. Besides, agents' varying response preferences and independent awareness also pose significant difficulties for this task.

Huazhong University of Science and Technology, Wuhan, Hubei, P.R.China. Email:{conghao\_wong, xbh\_hust, pengqinmu, yuanwei, youxg}@hust.edu.cn



Fig. 1. Agents' personalities and preferences may be affected by a large number of hidden factors, thus presenting a variety of future *behavior styles*. When we do not kow much about the target agents or their behavior preferences, a natural thought is to sequentially assume that they behave with the specific behavior style. Then, we could predict its all potential future choices under these assumptions, thus giving a series of future predictions with significant style differences. We call this strategy as the *Multi-Style Prediction*.

Previous researchers have studied two main factors that affect agents' future plannings, i.e., the social interaction (also called the agent-agent or human-human interaction) [13], [14] and the scene interaction (agent-scene interaction) [15], [16]. They give agents socially and physically acceptable predictions by taking these interactive factors into account. In addition, other researchers like [14], [15] have widely studied stochastic prediction methods to reflect agents' uncertain future choices and multi-path preferences. However, few of them have differentiated modeled agents' behaviors. In other words, most current methods predict all agents' possible future choices with the same "style". Unlike agents' uncertainty, the "style" reflects the different preferences for making decisions and plans. Even for agents with almost the same past status, their future choices may have huge differences due to their different behavior styles. For example, a father and his boy get out together in the morning, while his boy may go to school at the crossroad like a "student", and the father may get to his company for he is an "employee". Although some stochastic methods aim to study and give agents multipath predictions, such hugely different future choices are still challenging to describe and analyze through random factors or samplings. It makes them challenging to reflect differences in agents' multiple future plannings and the potential intra-class behavioral differences among agents.

**Hidden Factors**. Most trajectory prediction methods encode agents' observed trajectories and surroundings to represent their behaviors in a "common" way. However, there exists something *behind the prediction scenes* that are hard to be described with specific metrics but plays a significant role in

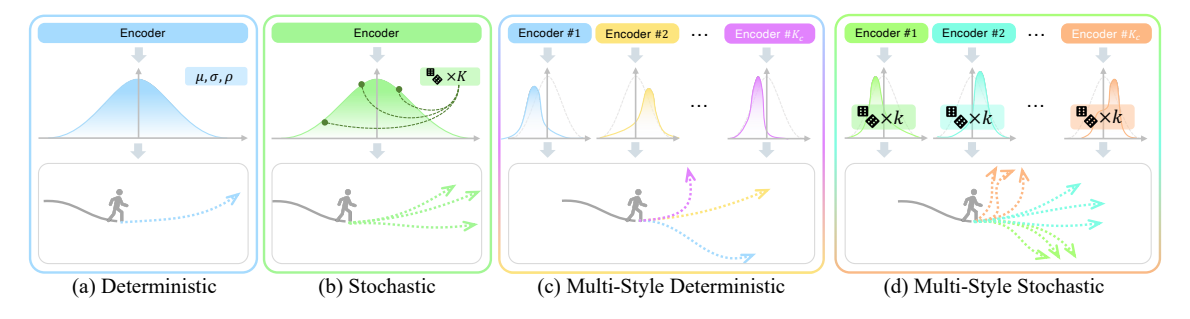


Fig. 2. Illustration of different kinds of prediction methods. (a) Deterministic methods predict the "average" trajectory from a specific distribution. (b) Stochastic methods provide N=K multiple trajectories by employing generative neural networks and randomly sampling vectors K times from the distribution. (c) and (d) show multi-style methods proposed in this study. (c) Multi-style deterministic method would give  $K_c$  "average" predicted trajectories from multiple categorized distributions via the corresponding generator or encoder. (d) Multi-style stochastic method would generate  $N=kK_c$  trajectories by sampling k random predictions from each categorized distribution.

affecting agents' plannings. Whether it is occupation, educational experience, or personality, all have a different impact on people's plans. These factors would determine agents' behaviors and plannings directly, so we call them the *hidden factors*. Whichever factor changes, their future plans may be different. As shown in Fig. 1, some hidden factors may make the person happy, sad, angry, or depressed, and some other factors make them become a doctor, a researcher, a policeman, and many other professions. All these will lead to a completely different future *behavior style*.

Behavior Categories && Multi-Style Prediction. It is difficult to determine and quantify these hidden factors. On the contrary, agents' trajectories can be observed and recorded easily. A natural thought is to establish a connection between agents' trajectories and these hidden factors, thereby reflecting the potential impact of these invisible factors on their future plannings categorically. Precisely, we classify agents' behaviors into several categories adaptively to reflect the coinfluence of hidden factors on their plannings, and employ a series of generators to learn to generate trajectories with the corresponding behavior styles separately. We call these categories the *Hidden Behavior Categories* since we do not know how each category's trajectories are distributed and presented. With the help of these categories, we can sequentially assume that the target agent may behave with the specific behavior style. Then, we employ the corresponding trajectory generator to give predictions under the corresponding style assumptions, thus obtaining a series of *Multi-Style* predictions. In this way, these generators could give a series of future predictions with sufficient differences in behavior styles. As shown in Fig. 1, we call the above prediction strategy the *Multi-Style Prediction*.

Multi-Style Prediction v.s. Stochastic Prediction. Some researchers have employed generative models, like Generative Adversarial Networks (GANs) [14], [15] and Variational Autoencoders (VAEs) [17], to study agents' uncertainty and randomness, and generate multiple random future predictions. These methods may encode agents' trajectories and interactive behaviors into a specific data distribution (like the normalized Gaussian distribution), and then randomly sample features to generate multiple random future choices. However, agents' style attributes may be compressed when they encode their behaviors into the "Non-categorized" latent space. Therefore,

these randomly sampled trajectories would lose their corresponding stylized semantics. It is difficult to provide a variety of predictions with sufficient style differences within limited samplings, not to mention the categorized predictions. Although some methods [7], [18] have tried to further model interactions by manually labeling trajectory classifications, they may consume a lot of labeling costs and may be challenging to adapt to a broader range of prediction scenarios. Different from most current stochastic methods, the multi-style prediction strategy will provide multiple predictions for the same agent in a multi-style way with the help of the above *Hidden Behavior* Categories. Different trajectory generators perform their duties within each category, respectively predicting future choices with different styles, so as to avoid the above problems and then adaptively provide multi-style predictions with significant categorical differences in parallel. See details in Fig. 2.

Multi-Style Prediction v.s. Goal-Oriented Prediction. In the above discussions, we try to model agents' multistyle characteristics by classifying them into several hidden behavior categories in an adaptive way. Inspired by recent goal-oriented methods like [19], we use agents' end-points plannings as one of the representative "features" to indicate each behavior category. It is a natural choice to utilize agents' end-point plannings along with their interactive status to reflect their behavior styles. For example, in the above boyfather case, we can infer the boy presents the behavior in a "student-like" style and the father in an "employee-like" style. These two behaviors present entirely different styles from their different end-points plannings. When another agent comes to the crossroad while we know nothing about it, we can assume that he may act like the above two styles. Then, two generators may give two different predictions, which contain a prediction to go to school with a "student-like" style and another to go to the company with an "employee-like" style. Please note that utilizing agents' end-points to classify their behavior styles does not mean that every agent in the same behavior category has similar end-point plans. Instead, we hope agents in the same category may represent similar interaction details and behavior preferences that can be "inferred" from their end-points. In short, we attempt to classify agents' behavior styles by considering their end-points plannings and interactive context, rather than classify their "destinations", which is quite

different from some goal-oriented methods like [20].

In this manuscript, we propose the multi-style network MSN to learn how the hidden factors categorically determine agents' behavior styles through their end-point plannings and the interactive context, and utilizes  $K_c$  style channels to give agents multiple future predictions with sufficient style differences. We first classify agents' trajectories along with their interactive video context into several hidden behavior categories according to their end-points plannings adaptively. Then, we employ and train a generator with a series of style channels to learn how agents' behavior representations distribute in each style and then give multiple stylized planning hypotheses. We will finally implement the stylized predictions based on the given planning hypotheses in each style channel by considering agents' potential interactive behaviors. Our contributions are summarized as follows:

- We propose the novel *multi-style* prediction strategy, and employ two sub-networks, *style hypothesis* and *stylized prediction* sub-networks, to give agents multi-style predictions along with the novel *hidden behavior category* based stylized loss.
- We propose two Transformer-based networks, the deterministic MSN-D and the stochastic MSN-G, to reach the multi-style prediction goal from two ways.
- Experiments demonstrate that MSN outperforms current state-of-the-art methods on ETH-UCY and SDD, and show better multi-style characteristics.

## II. RELATED WORK

This manuscript focuses on categorically modeling agents' behaviors and predicting their future trajectories in a novel multi-style strategy. We summarize relevant trajectory prediction approaches containing trajectory categorization, stochastic trajectory prediction, and goal-driven trajectory prediction.

## A. Trajectory Prediction

There are a lot of previous studies [21] focusing on predicting agents' trajectories in crowded spaces. Alahi et al. [13] treat this task as the sequence-data generation problem, and adopt one of the recurrent neural networks, Long Short-Term Memory (LSTM), to model agents' observed behaviors. It also considers the social interaction with the Social Pooling mechanism. After that, methods like Pooling [14], sorting [15], [16], Agent-aware Attention Mechanism [22]-[25] have been proposed to further model agents' social interactions and achieved great performance. In addition to the social interaction, some researchers have studied the physical constraints of scene objects on agents (named scene interactions). Methods like [26]–[28] utilize the Convolutional Neural Networks (CNNs) to extract scene semantics from RGB images or videos, therefore helping generate physically acceptable predictions. Moreover, [29]-[31] employ scenes' segmentation maps to model how different kinds of physical components affect agents' decisions. Besides, researchers also employ Graph Attention Networks (GATs) [22], [32], Graph Convolution Networks (GCNs) [33] and Transformers [34], [35] as their backbones to obtain better agent representations. Despite such a wealth of research, most methods utilize the "same" prediction strategy for all agents rather than providing stylized predictions. Style semantics may be compressed when encoding agents' behavior representations due to the "non-categorical" feature distributions. It means that it could not be easy for most current methods to reflect agents' different behavior styles in various heterogeneous prediction scenarios.

## B. Trajectory Categorization

Few methods have tried to model interactions in a refined manner through trajectory classification strategies. For example, Deo et al. [7] classify car motions into lane-passing, overtaking, cutting-in, and drifting-into-ego-lane maneuver classes for freeway traffic. Moreover, Kothari et al. [18] give the exact trajectory categorization method and divide pedestrian trajectories into static, linear, leader-follower, collision-avoidance, group, other interactions, and non-interacting categories when modeling social interactions. Kothari et al. [18]also annotate all the training data in the entire dataset into the above categories, thus achieving the purpose of learning interaction relationships and trajectory plannings categorically. Besides, Kotoari et al. [36] also divide agents' interactive behaviors into avoid-occupancy, keep-direction, leader-follower, and collision-avoidance.

However, these manual classification strategies may significantly increase the workload of model training, and they may be difficult to migrate to different trajectory prediction scenarios adaptively. Besides, most of these classification methods are proposed to better model interactive behaviors rather than agents' multiple future choices. This manuscript will try to achieve multi-style trajectory generation through a simple but effective trajectory classification strategy. We try to introduce an adaptive behavior classification method and train a series of generators to learn the corresponding behavior styles, therefore generating multiple predictions with quite different styles, which avoids potential problems caused by manual annotations.

## C. Stochastic Approaches

Researchers have recently paid more attention to modeling the multi-modal characteristics of agents' future choices, leading to a series of stochastic methods (also called generative or multi-modal methods). Generative networks, like VAEs [17], [37], and GANs [14]–[16], [38], are widely used to implement multiple random trajectories. Compared with previous single-output prediction methods (also named the deterministic models), the stochastic methods could better reflect agents' diverse preferences and uncertain future choices.

However, stochastic prediction methods consume more computational resources than the deterministic method since they have to repeat sampling and calculating to obtain multiple random predictions. Most importantly, these methods give multiple predictions with randomly sampling trajectories from the same distribution for all agents, resulting in a "single" prediction style. Although some models have tried to improve and use specific sampling methods, like the Truncation Trick [19] and the Test-Time Sampling Trick [39], using a "single"

4

distribution to describe the diverse and differentiated behavioral characteristics of agents may compress their personalized styles. In this way, these methods might ignore agents' multi-style characteristics, making them challenging to reflect agents' stylized future choices within limited samplings.

## D. Goal-Driven Approaches

The modeling of agents' intentions and goal plannings has been widely studied in robot navigation, path planning, autonomous vehicles, and many other tasks. Several researchers [19], [39]–[43] have started to bring them to the trajectory prediction task to explore agents' multiple future choices. Rehder et al. [40] propose a destination conditioned method to predict trajectories. After that, Rehder et al. [41] utilize a deep learning approach to handle intention recognition and trajectory prediction simultaneously. Mangalam et al. [19] propose the endpoint conditioned trajectory prediction method. and they try to address agents' random endpoint choices by gathering scene segmentation maps and agents' historical trajectories in [39]. Quan et al. [44] employ an extra intention LSTM cell to capture the intention cues and their changing trends. In addition, some methods use the scene context, such as scene images [20], [44], to infer their possible goal choices.

However, these methods may ignore the diversity of agents' future choices and differentiated destination planning preferences. Like most stochastic prediction methods, most of them may be challenging to generate predictions with significantly different future choices or destination plannings. Besides, these intention modules may be hard to adapt to more prediction scenarios due to the changing of scene appearances. Inspired by but different from these methods, we try to classify and model agents' behavior styles through their destination selections rather than modeling their goals or destinations separately. Then, we could model their possible future behaviors categorically and adaptively to avoid these possible problems while maintaining the performance improvement brought by these goal-driven approaches.

#### III. MSN

We focus on predicting agents' trajectories in crowd scenes with a novel multi-style way in this manuscript. We utilize two Transformer-based sub-networks, the *style hypothesis* and the *stylized prediction* sub-networks, to achieve the multi-style prediction goal with the help of the novel stylized loss. Fig. 3 shows the overall architecture of MSN, and Fig. 4 shows how the stylized loss works when training. Detailed structures of sub-networks or layers are listed in TABLE I.

## A. Problem Definition and Formulation

Given a video clip (a series of scene RGB images)  $\{I\}$  that contains  $N_a$  agents (e.g., pedestrians, vehicles, etc.) along with their observed trajectories during past  $t_h$  frames, trajectory prediction takes into account their motions and interactions as well as scene constraints to predict their future  $t_f$  frames' possible positions. Let  $p_t^i = (p_x^i, p_y^i) \in \mathbb{R}^2$  denote the position of agent-i at frame t. To distinguish coordinates at

TABLE I LAYERS USED IN THE PROPOSED MSN.

Layers	Structure
$\mathrm{MLP}_e$	$X \to \mathrm{fc}(d/2) \to \mathrm{tanh}() \to f_t$
MID	$C \to \text{AvgPooling}(5 \times 5) \to \text{Flatten}()$
$MLP_c$	$\rightarrow \mathrm{fc}(dt_h) \rightarrow \mathrm{tanh}() \rightarrow \mathrm{Reshape}(t_h \times d) \rightarrow f_c$
Tuon	$f \to \text{TransformerEncoder } (d) \to f1;$
Tran <sub>b</sub>	$f1, X \to \text{TransformerDecoder } (d) \to \text{fc}(d) \to h_{\alpha}$
G	$h_{\alpha} \to K_c \times \text{Conv}(1 \times t_h) \to \text{fc}(d) \to F;$
G	$F \to \tanh() \to \mathrm{fc}(2) \to D$
TD.	$f_k \to \text{TransformerEncoder}(d) \to f_2;$
${ m Tran}_i$	$f_2, \hat{Y}_l, X \to \text{TransformerDecoder}(d) \to h_\beta$
$MLP_d$	$h_{eta}  ightarrow \mathrm{fc}(2)  ightarrow \hat{Y}_D$
MID	$\operatorname{Concat}(h_{\beta}, z) \to \operatorname{fc}(d) \to \operatorname{ReLU}() \to g1;$
$MLP_g$	$\operatorname{Concat}(h_{eta},z)+g1  o \operatorname{fc}(2)  o \hat{Y}_g$

observation and prediction periods, we denote  $x_t^i = p_t^i$  when  $1 \leq t \leq t_h$ , and  $y_t^i = p_t^i$  when  $t_h + 1 \leq t \leq t_h + t_f$ . Agent-i's observed trajectory can be written as  $X^i = \left\{x_t^i\right\}_{t=1}^{t_h}$ , and the future groundtruth trajectory as  $Y^i = \left\{y_t^i\right\}_{t=t_h+1}^{t_h+t_f}$ . Trajectory prediction focused in this study is to predict agents' possible future positions  $\mathcal{Y} = \{\hat{Y}^i\}_{i=1}^{N_a}$  according to their observed trajectories  $\mathcal{X} = \{X^i\}_{i=1}^{N_a}$  and the scene context gotten from RGB image I. The subscript i, which denotes the agent's index, will be omitted for a simple expression.

#### B. Style Hypothesis

The style hypothesis sub-network aims to model agents' various behavior styles into several *Hidden Behavior Categories*, and then give planning hypotheses by assuming they may behave like each of the potential behavior styles. We introduce this stage from the following aspects, i.e., representations for different agents, the categorical modeling of their behavior styles, and the hypotheses for their potential styles.

a. Agent Representations and Behavior Features Agents always consider both their current status and the surroundings to plan their activities. Following [45], we use agents' observed trajectories and their context maps  $^1$  together to represent their interactive status. We employ an MLP named MLP<sub>e</sub> (see details in TABLE I) to embed agent's observed trajectory X into the d/2 dimensional feature. Similarly, we take another MLP (MLP<sub>c</sub>) to model interactions into the context feature  $f_c$ . We obtain the agent representation by concatenating these two features. Formally,

$$C = \text{CNN}(\mathcal{X}, I),$$

$$f_t = \text{MLP}_e(X) \in \mathbb{R}^{t_h \times d/2},$$

$$f_c = \text{MLP}_c(C) \in \mathbb{R}^{t_h \times d/2},$$

$$f = \text{Concat}(f_t, f_c) \in \mathbb{R}^{t_h \times d}.$$
(1)

We employ a Transformer-based<sup>2</sup> behavior encoder (Tran<sub>b</sub>) to infer agents' behavior features  $h_{\alpha}$  from their representations f and the observed trajectories X. Please see TABLE I and Appendix A for the detailed Transformer settings. Formally,

$$h_{\alpha} = \operatorname{Tran}_{b}(f, X) \in \mathbb{R}^{t_{h} \times d}.$$
 (2)

 $<sup>^{1}</sup>$  [45] proposes the context map C, and it is computed through the scene RGB images I via a CNN. Please see Appendix B for the qualitative analysis.  $^{2}$ Please see the detailed Transformer structure in Appendix A.

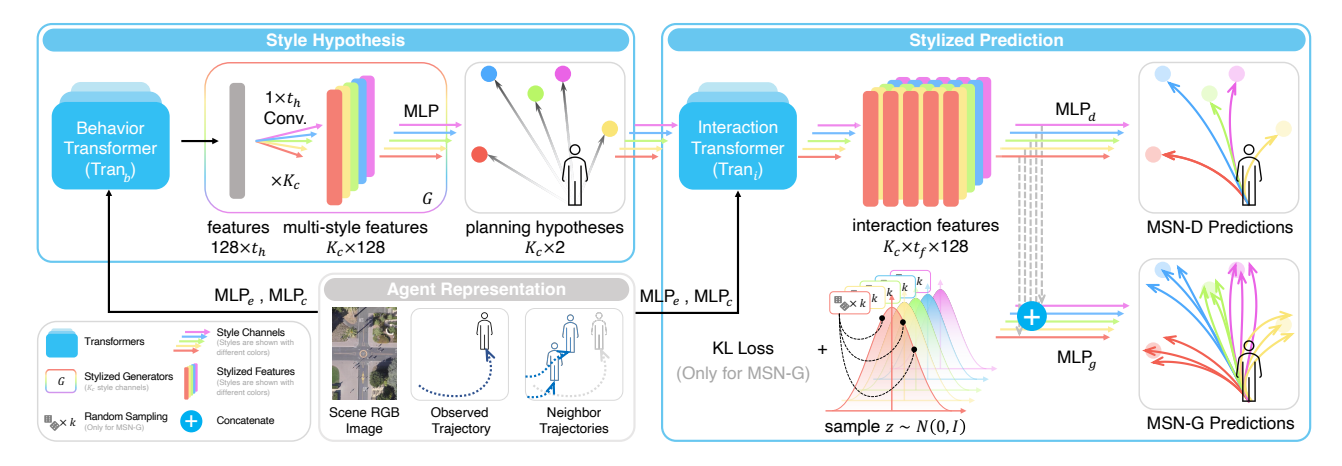


Fig. 3. MSN Overview. It contains two main sub-networks, the style hypothesis and the stylized prediction sub-network. Both the two sub-networks work together to give multi-style future predictions via  $K_c$  style channels (shown with arrows and features in different colors). Each of the stylized prediction is obtained through the inference of the corresponding style channel. We also propose the stochastic MSN-G to represent agents' random future choices.

**b. Hidden Behavior Categories** We try to model agents' multi-style characteristics by utilizing an adaptive way to classify all prediction samples into several *Hidden Behavior Categories*. As we have discussed in section I "INTRODUC-TION", agents' activities could be affected by various hidden factors. In addition, the "style" indicates a kind of continuously changing preferences, which means that it is challenging to classify their behaviors into discrete categories directly. Inspired by recent *goal-oriented* trajectory prediction methods, we take the *end-points* as the important manifestations to characterize agents' behavior styles. We regard that agents with almost the same observations, interactive context, and similar end-points plannings have the same behavior style.

We introduce a simple but effective similarity measurement method to judge whether different prediction samples (with the same observations and interactive context) belong to the same category. We distinguish their categories by finding the endpoint  $D_s$  from a set of other end-points  $D = \{(d_{ix}, d_{iy})\}_i$  that makes the Euclidean distance between the target end-point  $d = (d_x, d_y)$  and  $D_s$  reach the minimum value. Then, the target trajectory and the trajectory with end-point  $D_s$  are regarded as the same hidden behavior category. Formally,

Category
$$(d|D)$$
 = Category $(D_s)$ ,  
where  $s = \underset{i}{\operatorname{arg min}} ||D_i - d||_2$ . (3)

It is a relative classification strategy, which can be adapted to various prediction scenarios and agents with different behavior preferences. In addition, the minimum operation also saves complicated work like setting and verifying thresholds.

c. Style Hypothesis In order to directly give predictions with significant stylistic differences, we employ a set of generators  $G = \{G_1, G_2, ..., G_{K_c}\}$  to generate predictions with different styles correspondingly. Each generator could focus on different patterns that lead to the specific behavior style rather than the "common" behavior representations. Therefore, G could generate stylized predictions in parallel without any random sampling steps. We employ  $K_c$  convolution kernels  $\mathcal{K} = \{k_i\}_{i=1}^{K_c}$  (shape  $= 1 \times t_h$ ) as well as their corresponding

MLPs to generate the multi-style features from agents' behavior features. Convolution operations are applied on behavior features  $h_{\alpha}$  to obtain features from  $K_c$  channels (marked as F) with strong discriminative categorical styles. Formally,

$$F = \text{MLP}\left(\text{Conv}(h_{\alpha}^T, \mathcal{K})\right) \in \mathbb{R}^{K_c \times d}.$$
 (4)

Another decoder MLP is employed to infer the multi-style planning (end-point) hypotheses *D*. Formally,

$$D = \mathrm{MLP}(F) \in \mathbb{R}^{K_c \times 2}.$$
 (5)

We combine the above convolution layers and MLPs as the multi-style hypothesis generator G, which contains  $K_c$  style channels due to the convolution operation, and each channel can be regard as a stylized generator  $G_k$ . Formally, we have the planning hypotheses D in parallel:

$$D = \{D_1, D_2, ..., D_{K_c}\} = G(h_\alpha, \mathcal{K}) \in \mathbb{R}^{K_c \times 2},$$
 (6)

where  $D_k$   $(1 \le k \le K_c)$  represents the end-point hypothesis that output from the k-th style channel. We assign the category of the end-point hypotheses generated through k-th style channel as k. Formally,

$$Category(D_k) = k. (7)$$

Given the joint distribution (marked with  $\mathcal{D}_k$ ) of predictions  $D_k$  and groundtruths d that are classified into the k-th style, the k-th generator  $G_k$  will be trained through the corresponding k-th stylized loss function  $\mathcal{L}_{sty}(k)$ . It aims to minimize the Euclidean distance between predictions and groundtruth that belong to the same hidden behavior category. Formally:

$$\mathcal{D}_{k} = P\left(D_{k}, d \mid \text{Category}(d|D) = k\right),$$

$$\mathcal{L}_{sty}(k) = \mathbb{E}_{(D_{k}, d) \sim \mathcal{D}_{k}} \|D_{k} - d\|_{2}.$$
(8)

As shown in Fig. 4, the style hypothesis sub-network (with  $K_c$  style channels) will be trained with the stylized loss. They learn how to classify samples into  $K_c$  hidden behavior categories adaptively, learn how each category's behavior features distribute, and further learn different behavior patterns that different style channels should focus on. Finally, the subnetwork gives multiple planning hypotheses with  $K_c$  quite different styles in parallel with these  $K_c$  style channels.

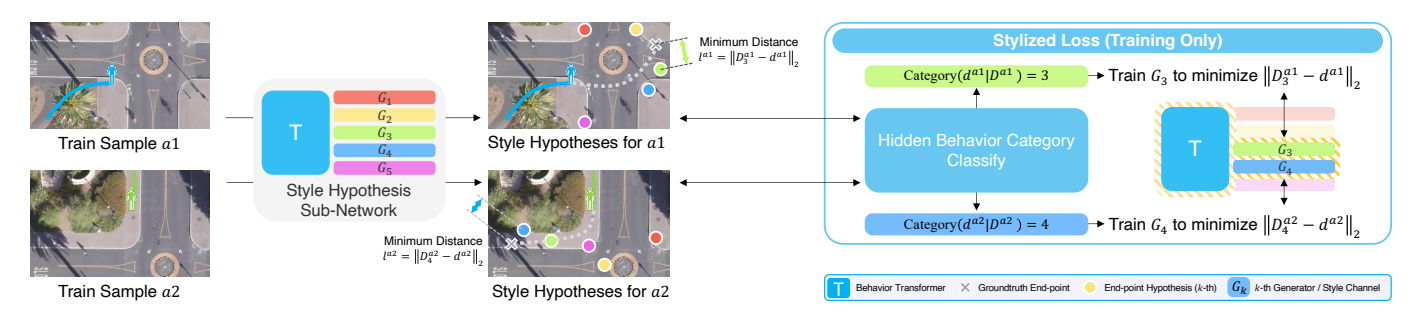


Fig. 4. Illustration of the multi-style planning hypothesis sub-network and the stylized loss. In the style hypothesis stage, the sub-network infers agents'  $K_c$  ( $K_c = 5$  in the above schematic figure) possible future behavior styles via their future goal plannings with the corresponding stylized generator (style channel). When training the network, we classify sample into k-th category by judging which channel makes the Euclidean distance between the predicted  $D_k$  and the groundtruth d reach the minimum value. The stylized loss is used to minimize the above minimum distance by tuning trainable parameters in the behavior Transformer and the corresponding  $G_k$ . It makes sure that different generators  $\{G_k\}_{k=1}^{K_c}$  could give multiple hypotheses with quite different styles.

## C. Stylized Prediction

The stylized prediction sub-network aims to give complete predictions under the given multi-style end-points hypotheses and the interaction details. It also takes agents' uncertainty into account and gives stochastic predictions in the MSN-G. a. Interaction Features Similar to Equation 1, we take agents' observed trajectories X and context maps C to represent their status and interactions. We expand the number of time steps from  $t_h$  into  $t_h + 1$  to fit the stylized planning hypotheses. For the k-th planning hypothesis  $D_k$ , we have the agent representation  $f_k$ :

$$\begin{split} f_{tk} &= \mathrm{MLP}_e(\mathrm{Concat}(X, D_k)), \\ f_{ck} &= \mathrm{MLP}_c(t_h = t_h + 1)(C), \\ f_k &= \mathrm{Concat}(f_{tk}, f_{ck}) \in \mathbb{R}^{(t_h + 1) \times d}. \end{split} \tag{9}$$

Similar to the above behavior features, we take the Transformer as the backbone of the interaction encoder (Trans $_i$ ) to obtain interaction features. When an agent has specific future planning and no other restrictions, the natural plan is to move towards its destination straightly. Other factors affecting its movement can be considered as an embodiment of interactive behaviors. We use the linear spatio-temporal interpolation sequence between agents' current positions (the last observed point) and the given planning hypothesis as one of the inputs to model these interactive behaviors. Formally, the linear sequence  $\hat{Y}_k^l$  and the interaction feature  $h_{\beta_k}$  are computed from the k-th style channel as:

$$\hat{Y}_{k}^{l} = \left\{ x_{t_{h}} + \frac{t}{t_{f}} (D_{k} - x_{t_{h}}) \right\}_{t=1}^{t_{f}} \in \mathbb{R}^{t_{f} \times 2},$$

$$h_{\beta_{k}} = \operatorname{Tran}_{i}(f_{k}, X, \hat{Y}_{k}^{l}) \in \mathbb{R}^{t_{f} \times d}.$$
(10)

Finally, the  $\operatorname{Tran}_i$  outputs the multi-style interaction features  $h_\beta = \left(h_{\beta_1}, h_{\beta_2}, ..., h_{\beta_{K_c}}\right) \in \mathbb{R}^{K_c \times t_f \times d}$  from the corresponding style channels (all channels' weights are shared).

**b. Multi-Style Prediction** We provide two kinds of MSN, the deterministic MSN-D and the stochastic MSN-G, to handle different prediction scenarios.

**MSN-D**: We employ an MLP (MLP<sub>d</sub>) to obtain the multistyle deterministic 2D-coordinate prediction sequences  $\hat{Y}_D$ from the interaction features  $h_\beta$ . Formally,

$$\hat{Y}_D = \text{MLP}_d(h_\beta) \in \mathbb{R}^{K_c \times t_f \times 2}.$$
 (11)

Like the style hypothesis sub-network, trajectories with different styles are implemented via different style channels (wights are shared). Then, MSN-D could give  $N=K_c$  multiple predictions with  $K_c$  styles from one implementation without any repeated sampling operations.

**MSN-G**: The deterministic MSN-D could not reflect agents' uncertainty or randomness when making decisions. We expand the original MLP<sub>d</sub> into the MLP<sub>g</sub> to generate stochastic predictions *within* each hidden category to bring it randomness factors. The MSN-G will be trained with the addition KL loss, thus allowing it to give random predictions via the noise vector. Given a random sampled vector  $z \sim N(0, I)$ , we have:

$$\hat{Y}_g = \text{MLP}_g(h_\beta, z) \in \mathbb{R}^{K_c \times t_f \times 2}.$$
 (12)

After repeating for k times, we have the stochastic predictions  $\hat{Y}_G = (\hat{Y}_{g1}, \hat{Y}_{g2}, ..., \hat{Y}_{gk}) \in \mathbb{R}^{k \times K_c \times t_f \times 2}$ . MSN-G has  $K_c$  style channels, and it could output  $N = kK_c$  trajectories after k times of random sampling.

## D. Loss Functions

We train the MSN end-to-end with the loss function:

$$\mathcal{L}_{MSN} = \underbrace{\mathcal{L}_{sty}}_{stage 1} + \underbrace{\mu_1 \mathcal{L}_{ad} + \mu_2 \mathcal{L}_{diff} + \mathcal{L}_{kl}}_{stage 2}.$$
 (13)

**Stylized Loss**  $\mathcal{L}_{sty}$  is used to train the stage 1 sub-network, making each of the style channel available to output planning hypotheses with quite different behavior styles. See detailed explanations in Equation 3 and Equation 8. Formally,

$$\mathcal{L}_{\text{Stv}} = \mathbb{E}_{k \sim P(k)} \mathcal{L}_{sty}(k). \tag{14}$$

Average Displacement Loss  $\mathcal{L}_{ad}$  is the average point-wise displacement for each predicted point. Formally,

$$\mathcal{L}_{ad} = \frac{1}{N_a t_f} \sum_{i} \sum_{t} ||y_t^i - \hat{y}_t^i||_2.$$
 (15)

TABLE II Comparisons with the best-of-20 validation. Metrics are shown with "ADE/FDE". Lower means better.

Models	eth	hotel	univ	zara1	zara2	Average
Social GAN [14]	0.60/1.19	0.52/1.02	0.44/0.84	0.22/0.43	0.29/0.58	0.41/0.81
SoPhie [15]	0.70/0.43	0.76/1.67	0.54/1.24	0.30/0.63	0.38/0.78	0.54/1.15
Social-BiGAT [16]	0.69/1.29	0.49/1.01	0.55/1.32	0.30/0.62	0.36/0.75	0.48/1.00
Next [29]	0.73/1.65	0.30/0.59	0.60/1.27	0.38/0.81	0.31/0.68	0.46/1.00
PECNet [19]	0.54/0.87	0.18/0.24	0.35/0.60	0.22/0.39	0.17/0.30	0.29/0.48
TPNMS [30]	0.52/0.89	0.22/0.39	0.55/0.13	0.35/0.70	0.27/0.56	0.38/0.73
E-SR-LSTM [25]	0.44/0.79	0.19/0.31	0.50/1.05	0.32/0.64	0.27/0.54	0.43/0.67
TP [35]	0.61/1.12	0.18/0.30	0.35/0.65	0.22/0.38	0.17/0.32	0.31/0.55
Trajectron++ [46]	0.43/0.86	<b>0.12</b> /0.19	0.22/0.43	0.17/0.32	0.12/0.25	0.20/0.39
LB-EBM [47]	0.30/0.52	0.13/0.20	0.27/0.52	0.20/0.37	0.15/0.29	0.21/0.38
MSN-D (Ours)	0.28/0.44	0.11/0.17	0.28/0.48	0.22/0.36	0.18/0.29	0.21/0.35
MSN-G (Ours)	0.27/0.41	0.11/0.17	0.28/0.48	0.22/0.36	0.18/0.29	0.21/0.34

Models	Social GAN	SoPhie	Multiverse [48]	SimAug [31]	PECNet	LB-EBM	MSN-D (Ours)	MSN-G (Ours)
SDD	27.25/41.44	16.27/29.38	14.78/27.09	12.03/23.98	9.96/15.88	8.87/15.61	7.69/12.39	7.68/12.16

**Differential Displacement Loss**  $\mathcal{L}_{\text{diff}}$  is the weighted sum of point-wise displacement among several orders' difference of predicted trajectories and groundtruths. It penalizes the high-order difference error between the predicted value and the actual trajectory sequence, which extends the average distance loss. It is employed to further "smooth" predictions. Let  $\Delta$  denote the differential operation. Given the number P and a set of balance coefficients  $\lambda_p$  (p=1,2,...), we have:

$$\Delta y_{t}^{i} = y_{t+1}^{i} - y_{t}^{i}, \quad \Delta^{0} y_{t}^{i} = y_{t}^{i},$$

$$\Delta^{p+1} y_{t}^{i} = \Delta (\Delta^{p} y_{t}^{i}) = \Delta^{p} y_{t+1}^{i} - \Delta^{p} y_{t}^{i},$$

$$\mathcal{L}_{diff} = \frac{1}{N_{a} t_{f}} \sum_{i} \sum_{t} \lambda_{p} \sum_{p=1}^{P} \|\Delta^{p} y_{t}^{i} - \Delta^{p} \hat{y}_{t}^{i}\|_{2}.$$
(16)

**KL** Loss  $\mathcal{L}_{kl}$  is the KL divergence between the distribution of agent features  $h_{\beta}$  (denoted by  $P_{\beta}$ ) and the normalized Gaussian distribution N(0, I). Formally,

$$\mathcal{L}_{kl} = D_{kl}(P_{\beta}||N(0,I)), \tag{17}$$

where  $D_{kl}(A||B)$  denotes the KL Divergence between distribution A and B. It is used to train the MLP $_q$  in MSN-G only.

## IV. EXPERIMENTS

#### A. Datasets

We evaluate MSN on three public available trajectory datasets, including ETH [3], UCY [49], and Stanford Drone Dataset (SDD) [50]. They contain trajectories with rich social and scene interactions in various heterogeneous scenarios.

**ETH-UCY Benchmark.** The ETH-UCY benchmark has been widely used to evaluate prediction performance. It contains five video clips in several different scenarios: eth and hotel from ETH, and univ, zara1, zara2 from UCY. Its annotations are pedestrians' real-world coordinates (in meters) with a specific sampling interval. We follow the widely used "leave-one-out" strategy in previous studies [13], [14] when training and evaluating the proposed methods on ETH-UCY.

Stanford Drone Dataset. The Stanford Drone Dataset (SDD) [50] is a popular dataset used for object detection, tracking, trajectory prediction, and many other computer vision tasks. A lot of recent state-of-the-art trajectory prediction methods [19], [31] start to evaluate their ideas on it. It contains 60 bird-view videos captured by drones over Stanford University. Positions of more than 11,000 different agents with various physical types, e.g., pedestrians, bicycles, and cars, are given through bounding boxes in pixels. It has over 185,000 interactions between agents and over 40,000 interactions among agents and scene objects [50]. Compared with ETH-UCY, it has a richer performance in interaction complexity and differences in scene appearance or structure. Dataset split used to train MSN on SDD (dividing the total 60 SDD videos into 36 training videos, 12 validation videos, and 12 test videos) comes from [31], [48] (can be found at https://github.com/JunweiLiang/Multiverse).

#### B. Implementation Details

We train and evaluate our model by predicting agents' future coordinates in  $t_f = 12$  frames according to their observed  $t_h = 8$  frames' coordinates along with the video context. The frame rate is set to 2.5 fps, i.e., the sample interval is set to  $\Delta t = 0.4$ s. We train the entire network with the Adam optimizer with a learning rate lr = 0.0003 on one NVIDIA Tesla P4 graphic processor. In detail, we train MSN 800 epochs on ETH-UCY, and 150 epochs on SDD. When making training samples, we use a rectangular sliding window with the bandwidth = 20 frames and stride = 1 frame to process original dataset files to obtain training samples [14]. The feature dimension is set to d = 128. Detailed layers' structures and activations are listed in TABLE I. Detailed Transformer settings are shown in Appendix. The number of hidden behavior categories is set to  $K_c=20$  to align with the best-of-20 validation when compared to other multiple output methods. We set P=2 in the differential displacement loss, and take their coefficients as  $\lambda_1 = 0.5, \lambda_2 = 0.05$ . Balance coefficients used in the loss function is set to  $\{\mu_1, \mu_2\} = \{0.8, 0.2\}$ .

## C. Metrics and Baselines

We use the Average Displacement Error (ADE) and the Final Displacement Error (FDE) to measure network performance with the *best-of-20* validation [14], which takes the minimum ADE and FDE among 20 predictions to measure prediction accuracy. ADE is the average point-wise  $\ell_2$  error between prediction groundtruth, and FDE is the  $\ell_2$  error of the last prediction point. For one prediction sample, we have:

ADE = 
$$\frac{1}{t_f} \sum_{t} \|y_t - \hat{y}_t\|_2$$
,  
FDE =  $\|y_{t_h + t_f} - \hat{y}_{t_h + t_f}\|_2$ . (18)

We choose several state-of-the-art methods as our baselines:

- Social GAN [14]: A GAN-based model that considers social interaction to give stochastic predictions.
- **SoPhie** [15]: A GAN-based model that considers the physical constraints of the scene when predicting.
- Social-BiGAT [16]: A GAN-based model that combines Bicycle-GAN and Graph Attention Networks to model agents' stochastic nature.
- Next [29]: A model that aims to predict pedestrians' future paths jointly with their activities by multitask learning.
- **Multiverse** [48]: A model that focuses on predicting the distribution over multiple possible future paths of people as they move through various visual scenes.
- **SimAug** [31]: A model that aims at mixing the hardest camera view with the original view's adversarial feature to learn robust representations.
- **PECNet** [19]: A model that infers distant trajectory endpoints to assist in long-range multi-modal prediction.
- **TPNMS** [30]: A model that builds a feature pyramid with increasingly richer temporal information to capture agents' motion behavior at various tempos.
- **E-SR-LSTM** [25]: An extended version of SR-LSTM [24] exploits spatial-edge LSTMs to enhance the capacity to give multiple predictions.
- TP [35]: A Transformer-based "simple" model that predicts each person separately without any complex interaction terms but reaches great performance.
- **Trajectron++** [46]: A recurrent-graph-based model that aims at catching dynamic constraints such as moving agents and scene information.
- **LB-EBM** [36]: A probabilistic cost model accounts for movement history and social context in the latent space.

#### D. Comparison to State-of-the-Art Methods

This manuscript proposes two networks, the deterministic MSN-D and the stochastic MSN-G. It should be noted that we choose  $K_c=20$  as the basic configuration to meet the best-of-20 validation. It means that the stochastic MSN-G only samples k=1 trajectory from each style channel when outputs 20 predictions. Therefore, the reported results of MSN-D and MSN-G are "similar" in TABLE II. In this section,

we only discuss the MSN-D performance. For detailed results and stochastic performance about MSN-G, please refer to the section IV-E "Stochastic Performance".

**ETH-UCY.** Results in TABLE II show that the multi-style deterministic MSN-D outperforms a large number of current state-of-the-art models. We choose state-of-the-art stochastic models Trajectron++ [46] and LB-EBM [36] for comparison. Compared with Trajectron++, MSN-D significantly improves the ADE and FDE on eth sub-dataset for over 34.8% and 48.8%, and on hotel sub-dataset for 25.0% and 10.5%. Compared with Trajectron++ and LB-EBM, the average ADE is basically at the same level, but the average FDE of our proposed model gains about 10.2% on ETH-UCY. Note that MSN-D is *deterministic*, even if it could output  $N=K_c=20$  multi-style predictions at the same time. It still lacks uncertain factors when implementing. Nevertheless, its results on ETH-UCY show strong competitiveness even with other stochastic models when outputting the same number of trajectories.

**SDD.** As shown in TABLE II, MSN-D outperforms current state-of-the-art LB-EBM on the average ADE/FDE on SDD by a significant margin of 13.3% and 20.6%. Besides, it has dramatically improved ADE by over 22.8% and FDE over 22.0% compared with PECNet. As a result, the deterministic MSN-D performs better than most of the other stochastic models on SDD under the *best-of-20* validation. It reflects the superiority of MSN-D in handling complex data since SDD contains more heterogeneous agents and scenarios.

#### E. Quantitative Analysis

To explore the overall effect of the two sub-networks, we run several ablation experiments and show quantitative results in TABLE III, TABLE IV, and Fig. 5.

a. Style Hypothesis. The style hypothesis sub-network gives  $K_c$  styles of end-point hypotheses. As shown in TABLE III, the average error (FDE) of the hypothesized end-points even outperforms several current state-of-the-art methods (by the best-of-20 validation). Please note that we do not calculate ADE for study No. 1, for it only outputs end-points rather than the entire trajectories. Furthermore, study No. 2 demonstrates that its performance is even comparable to PECNet [19] with a considerable performance improvement (approximately 0.05 meters on ADE). Please note that study No. 2 only uses simple linear interpolation to obtain the entire predictions but considers nothing about agents' interactive behaviors. It shows the excellent performance improvement brought by the stage 1 style hypothesis sub-network. Compared to the state-ofthe-art goal-driven PECNet, we classify agents into several hidden behavior categories and then give multiple predictions by assuming agents would behave as each style in parallel, rather than randomly sampling trajectories for 20 times to obtain different predictions. It powerfully shows the overall efficiency of the style hypothesis strategy as well as the multistyle prediction strategy. For further explanations, please refer to the section IV-F "Prediction Styles".

**b. Stylized Prediction.** We show the complete MSN-D results

TABLE III

ABLATION STUDIES: ADE AND FDE ON ETH-UCY. S1 AND S2 REPRESENT THE STYLE HYPOTHESIS AND THE STYLIZED PREDICTION. EXPERIMENT NO.1 COULD NOT CALCULATE ADE FOR IT ONLY IMPLEMENTS S1. RESULTS ARE SHOWN WITH THE BEST-OF-20 VALIDATION.

No.	S1	S2	eth	hotel	univ	zara1	zara2	Average
1	<b>√</b>		NA/0.54	NA/0.19	NA/0.52	NA/0.36	NA/0.29	NA/0.38
2	✓	Linear	0.32/0.54	0.13/0.19	0.30/0.52	0.24/0.36	0.19/0.29	0.23/0.38
3	✓	✓	0.28/0.44	0.11/0.17	0.28/0.48	0.22/0.36	0.18/0.29	0.21/0.35

TABLE IV VERIFYING OF  $K_c$  in MSN-D and k in MSN-G. Metrics are shown with "ADE/FDE".  $N=kK_c$  denotes the number of output trajectories. Results with \* are relative values compared to the MSN-D ( $K_c=1$ ). Lower values indicate better performance.

	k	$K_c$	N	eth	hotel	univ	zara1	zara2	ETH-UCY	SDD	ETH-UCY*	SDD*
	-	1	1	0.65/1.27	0.23/0.42	0.62/1.23	0.46/0.91	0.41/0.81	0.47/0.93	16.76/32.83	100%/100%	100%/100%
	-	5	5	0.43/0.80	0.15/0.25	0.41/0.74	0.31/0.55	0.25/0.46	0.31/0.56	11.30/20.63	66%/60%	67%/63%
Ģ	-	10	10	0.37/0.65	0.13/0.21	0.36/0.65	0.28/0.47	0.22/0.37	0.27/0.47	9.52/16.60	57%/51%	57%/51%
MSN.	-	20	20	0.28/0.44	0.11/0.17	0.28/0.48	0.22/0.36	0.18/0.29	0.21/0.35	7.69/12.39	45%/38%	46%/38%
Σ	-	30	30	0.27/0.41	0.09/0.13	0.27/0.43	0.18/0.27	0.16/0.23	0.19/0.28	7.12/11.06	40%/30%	42%/34%
	-	50	50	0.24/0.33	0.09/0.11	0.22/0.32	0.17/0.22	0.14/0.19	0.17/0.23	7.13/10.86	36%/25%	43%/33%
	-	100	100	0.27/0.42	0.10/0.14	0.26/0.46	0.20/0.30	0.17/0.25	0.20/0.27	7.58/12.10	43%/29%	45%/37%
	1	20	20	0.27/0.41	0.11/0.17	0.28/0.49	0.23/0.36	0.18/0.29	0.21/0.34	7.98/12.96	45%/37%	47%/39%
Ϋ	5	20	100	0.20/0.27	0.08/0.11	0.23/0.37	0.18/0.24	0.14/0.20	0.16/0.23	5.83/7.93	34%/25%	34%/24%
MSN-G	10	20	200	0.19/0.22	0.08/0.09	0.22/0.33	0.16/0.21	0.13/0.17	0.15/0.20	5.27/6.49	32%/22%	31%/19%
Σ	20	20	400	0.18/0.18	0.07/0.07	0.20/0.29	0.15/0.18	0.13/0.15	0.14/0.17	4.86/5.30	30%/18%	28%/16%
	30	20	600	0.17/0.16	0.07/0.06	0.19/0.27	0.15/0.16	0.12/0.14	0.14/0.15	4.68/4.71	30%/16%	27%/14%

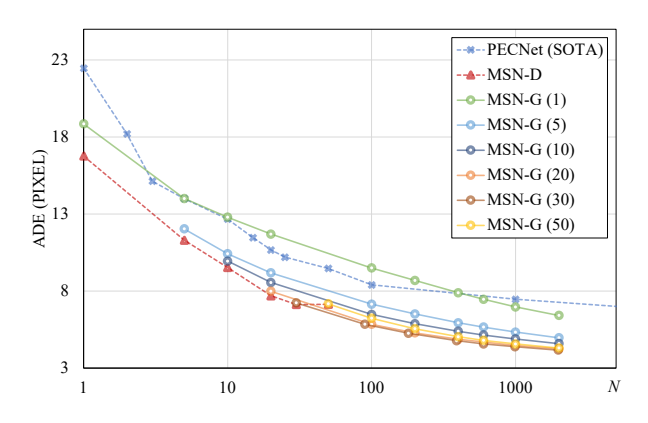


Fig. 5. ADE of MSN with different  $K_c$  and k configures on SDD.  $N=kK_c$  represents the number of predictions. Number in brackets represents  $K_c$ . The X-axis is shown in the log scale.

in TABLE III as study No. 3. Its ADE and FDE have improved over 7% compared with study No. 2, which utilizes linear interpolation and considers nothing about any interactions. It proves the effectiveness of the stylized prediction, which gives the entire trajectories under the given style's end-point considering agents' interactive behaviors. Besides, the most significant difference from No. 2 is that it brings better nonlinearity and sociality to the prediction with the help of the transformer skeleton. We will discuss more qualitative results in the section IV-F "Prediction Styles".

**c.** Verifying on  $K_c$ . The selection of the hyper-parameter  $K_c$  directly affects how MSN "judges" and classifies agents' potential behavior styles. A smaller  $K_c$  is not enough to

TABLE V Verifying of balance parameters in loss functions. We show the normalized results to reflect the performance changes.

_	No.	$\mu_1$	$\mu_2$	P	$\lambda_1$	$\lambda_2$	ADE*	FDE*
_	1	1.0	0.0	0	-	-	1.00	1.00
	2	0.5	0.5	1	1.0	-	1.05	1.08
	3	0.5	0.5	2	1.0	0.5	1.03	1.07
	4	0.5	0.5	2	0.5	0.05	1.01	1.03
	5	0.8	0.2	2	0.5	0.05	0.99	1.01

reflect agents' various behavior preferences. On the contrary, a larger  $K_c$  might require a large amount of training data to tune each generator to make them available to generate predictions with sufficient style differences. We run ablation experiments by verifying  $K_c$  in  $\{1, 5, 10, 20, 30, 50, 100\}$  to explore the multi-style performance on ETH-UCY and SDD. See details in TABLE IV. Results illustrate that MSN performs better with a higher  $K_c$  on both ETH-UCY and SDD when  $K_c$  is set to a relatively small value. Besides, it shows that setting  $K_c$  around 30-50 will lead to the best performance on each sub-datasets. On the contrary, a too-large  $K_c$  will cause performance degradation due to the limited training samples and behavior styles on ETH-UCY and SDD. It shows that the best  $K_c$  setting on ETH-UCY is about 50, and on SDD is about 30. Nevertheless, we still choose  $K_c = 20$  to adapt to the best-of-20 validation when comparing to other methods.

**d. Stochastic Performance.** The number of random generations k matters how the stochastic MSN-G performs. We present the comparison of MSN-G ( $K_c=20$ ) with several k settings in TABLE IV. To better show the stochastic



Fig. 6. Visualization of prediction styles. We show the first six styles of stylized predictions (yellow dots) for pedestrians a1 and a2 given by MSN-D ( $K_c = 20$ ). Their observations are shown with blue dots, and the given end-point hypotheses with green dots.

performance, we show the changing of ADE with different  $K_c$  and k configures on SDD in Fig. 5. We compare the proposed MSN-G with PECNet with the same number of output trajectories  $N=kK_c$ . It shows that MSN may achieve better performance with a lower N quickly. Compared with the goal-driven PECNet, MSN-G improves its ADE for over 41.4% when generating  $N=kK_c=1000$  trajectories. It illustrates MSN-G's advantages when generating a large number of predictions. It should be noted that when generating 1000 outputs, PECNet may sample trajectories for 1000 times. Meanwhile, the proposed MSN-G only takes 50 times of random sampling (when  $K_c=20$ ), which significantly improves the time efficiency of generating a large number of predictions.

In addition, it also shows the influence of  $K_c$  when generating the same number of trajectories. For example, results in Fig. 5 shows that MSN-G ( $K_c = 5, k = 4$ ) performs worse than MSN-G ( $K_c = 10, k = 2$ ) and MSN-G ( $K_c = 20, k = 1$ ), even they generate the same number  $(N = kK_c = 20)$  of trajectories. Besides, MSN-D ( $K_c = 100$ ) and MSN-G ( $K_c =$ 20, k = 5) also show the similar results in TABLE IV with about 10% performance difference. Both TABLE IV and Fig. 5 indicate that MSN may achieve best performance when setting  $K_c = 50$  on SDD, no matter how many stochastic predictions are generated. It means that the multi-style prediction strategy has a higher contribution in improving the model performance, and the random sampling in MSN-G makes it available to generate more trajectories easily and quickly to suit more application scenes. It also helps make the maximum use of computing resources. Note that we still choose  $K_c = 20$  and k=1 as the basic configuration when compared to other methods to in line with the best-of-20 validation.

e. Balance Parameters in Loss Functions. We use several different loss items (in Equation 13) to train the MSN. The stylized loss is used to train variables in stage 1 style hypothesis sub-network, and others are used together with parameters  $\{\mu_1, \mu_2\}$  to train variables in stage 2 stylized prediction subnetwork. The differential displacement loss also has hyperparameter P and a set of balance coefficients  $\{\lambda_1, \lambda_2, ..., \lambda_P\}$ . We train the MSN-D with different loss configures and run ablation experiments to show the performance comparison. Please note that the differential displacement loss and the stylized loss work on different sub-networks, which means that we could discuss the balance parameters used for training the stylized prediction sub-network separately. TABLE V shows their

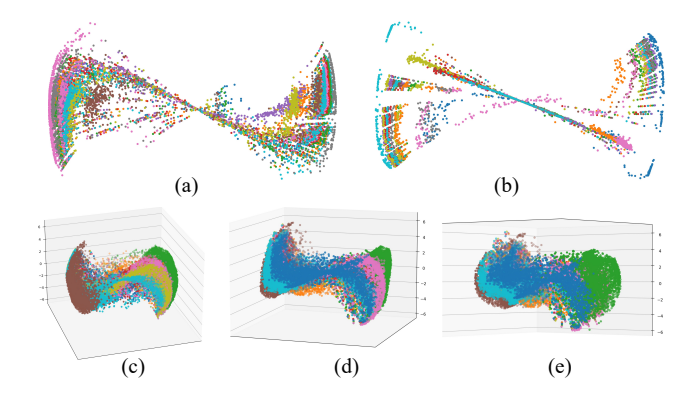


Fig. 7. Stylized Features. We show the 2D/3D feature distributions of the *d*-dimensional multi-style features via PCA. Each dot represents one stylized feature that belongs to a specific hidden behavior category. Categories are distinguished with colors. We show the 2D feature distributions on eth and zara1 in (a)(b), and the 3D distribution on univ with three views in (c)(d)(e).

quantitative results. It shows that the differential displacement loss does not significantly improve the quantitative prediction performance. On the contrary, an improper parameter ratio will degrade ADE or FDE. We insist on using this loss function to improve the predictions qualitatively, which could be difficult to be reflected directly by quantitative indicators like ADE or FDE. We will discuss how the differential displacement loss works qualitatively in the following section IV-F "Differential Displacement Loss".

#### F. Qualitative Analysis

a. Feature Visualization. We visualize several sampled agents' d-dimension multi-style behavior features  $F \in \mathbb{R}^{K_c \times d}$ to explore their distributions qualitatively. As shown in Fig. 7, all the features distribute on a low-dimensional manifold, and each category occupies a specific area in that manifold. In other words, the classification strategy adaptively divides the whole feature space into  $K_c$  parts according to their endpoint plannings and interactive context. Even though we do not know what these "styles" real meanings are, Fig. 7 shows that agents' behavior styles could be adaptively classified with such a simple minimum distance measurement. When we generate behavior features through the specific style channel, these features will naturally distribute in the corresponding style category. Furthermore, when generating multiple future predictions, we can selectively refer to the style priors rather than through the repeated random sampling like most existing

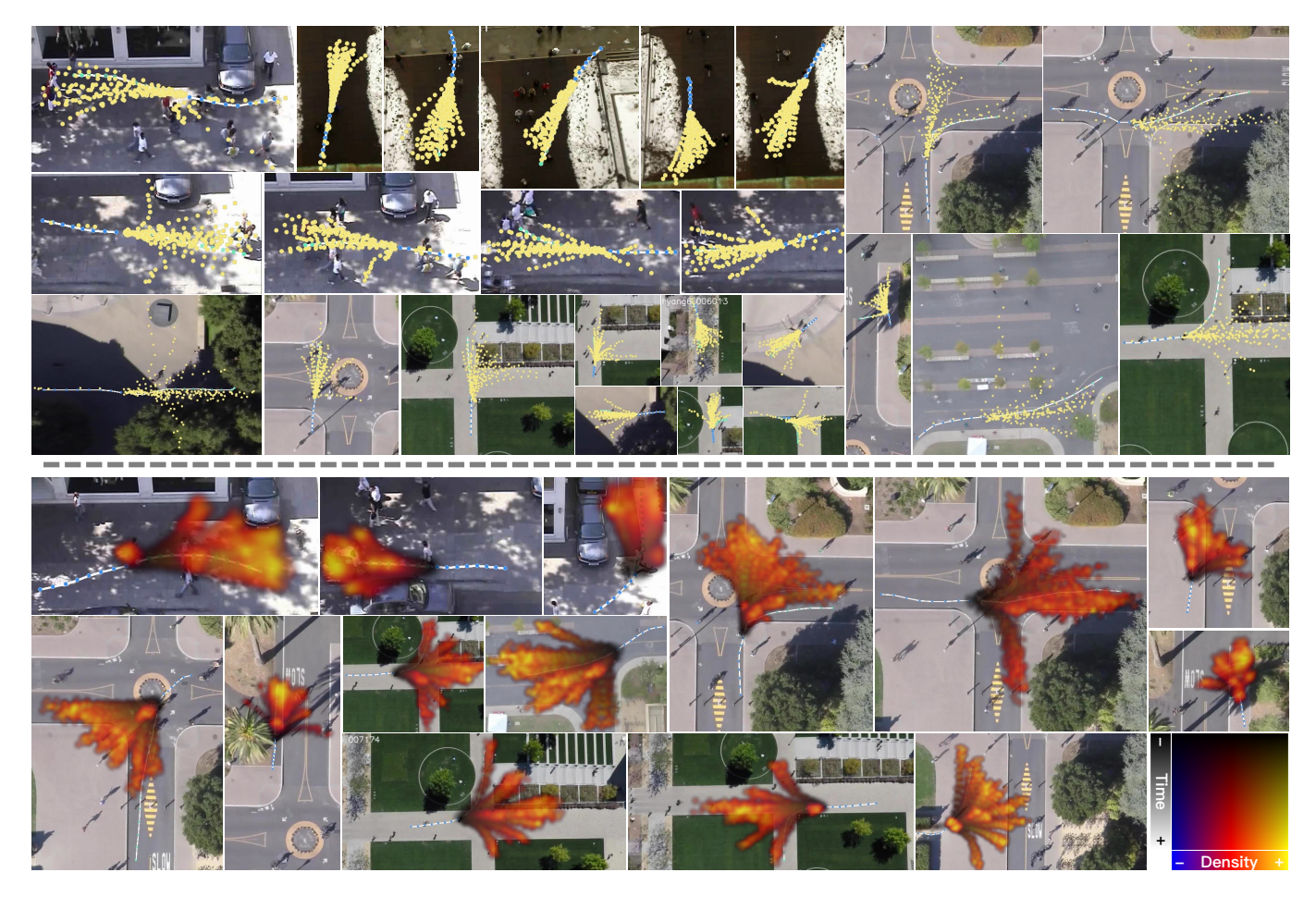


Fig. 8. Results visualization. We display visualized results of MSN-D ( $K_c = 20$ ) and MSN-G (shown with trajectory distributions) among several datasets. Bule dotes represent agents' observed trajectories, green dots are their groundtruths, and yellow dots are deterministic predictions given by MSN-D. For heatmaps given by MSN-G, yellow represents higher density and blue represent lower. Besides, time steps are distinguished with darker and lighter colors.

stochastic prediction models, which shows the efficiency of the adaptive classification strategy.

**b. Prediction Styles.** Another significant design is to predict trajectories in multiple style channels under their specific style hypotheses. Specifically, we take agents' end-point plannings as well as their interactive context to act as the reflection of their behavior styles, thereby utilizing  $K_c$  style channels to give the corresponding stylized predictions in parallel. We show several predictions given by different style channels for pedestrians a1 and a2 in Fig. 6. Predictions show that MSN has robust adaptability to different hypotheses and the possible agent-agent or agent-scene interactions. For example, it gives a1 and a2 predictions with various interactive behaviors like entering the shop (a2, channel 2), turning around (a1 and a2, channel 4), slowing down (a1 and a2, channel 6), and going around the parking car (a1, channel 2).

Besides, predictions within the same style channel show similar behavior trends and interactive behaviors. For example, style channel 1 gives the future predictions that both agent a1 and a2 may keep their current motion states and walk forward. The other style channel 2 considers they may have large-scale interactive behaviors to the scene context, and forecasts agent a1 to get through the parking car and turn around right

away and agent a2 to turn to the ZARA shop immediately. Similarly, channel 4 gives both predictions with quite drastic direction changes, and channel 6 thinks they may slow down in the future. Please note that we did not provide any style labels or annotations when training the whole network. It shows the effectiveness and strong adaptive ability of the proposed stylized loss and classification strategy for generating predictions with different behavior styles.

**c. Differential Displacement Loss.** The differential displacement loss is proposed to "smooth" trajectories, thus preventing the "unnatural" prediction cases. Compared with Fig. 9 (a) (b) (c) whose model is trained without the loss when training, results from Fig. 9 (d) (e) (f) looks more in line with the actual rules of pedestrian movements. The differential displacement loss will strengthen the constraints between each prediction point to obtain a prediction closer to the groundtruth while maintaining almost the same ADE. Unfortunately, there are still no metrics to describe the continuity of the predictions, which makes us difficult to compare with other methods.

## G. Limitations

Although the proposed MSN shows better performance, unexpected or failure predictions still exist in some output

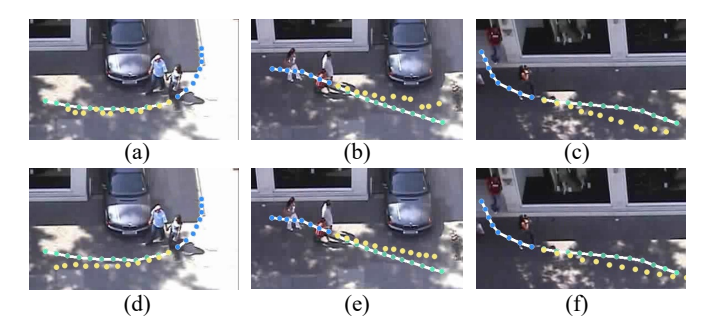


Fig. 9. Results comparison for the differential displacement loss. (a) (b) (c) are three prediction samples without the optimization of the differential displacement loss, and (d) (e) (f) are the corresponding predictions with the loss item when training. Blue dots, green dots, and yellow dots represent pedestrians' observations, groundtruths, and predictions, respectively.

style channels. In detail, it may have few (one or two out of twenty) style channels that give some unexpected stylized predictions in some datasets. For example, as shown in the first visualized prediction in the top-left of Fig. 8, several predictions almost coincide with the observed trajectory (but in the opposite direction). Although they almost do not affect the quantitative ADE and FDE under the best-of-20 validation, these predictions violate the physical limitations of agent activities. We speculate that this is due to the unbalanced training distribution that leads to the incomplete variables tuning in these style channels. This phenomenon occurs more in the ETH-UCY dataset but less in the SDD, which also verifies our point of view. We use a simple choosing strategy to suppress this problem temporarily. We discard all predictions  $\hat{Y}$  that satisfy  $\cos\langle X, Y \rangle < \cos(3\pi/4)$  to prevent this phenomenon temporarily. We will continue to study this problem and solve these failure categories in our future work.

#### H. Visualization

We display several prediction results of both MSN-D and MSN-G on ETH-UCY and SDD to show the performance qualitatively in Fig. 8. Blue dots represent the target agents' observed coordinates, and green dots are their groundtruth future coordinates. Yellow dots are deterministic predictions given by MSN-D (outputs totally  $N=K_c=20$  trajectories at once implementation), and heatmaps are the spatial distributions of the predicted trajectories given by MSN-G. Results show that the two-stage multi-style MSN has given multiple styles of predictions, such as pedestrians going ahead, turning around the crossroad, resting, and bicycles turning right or going ahead (but not turning left) at the roundabout. It is worth noting that in the prediction scene of the intersection shown in the bottom row in Fig. 8, our model gives a variety of future predictions with sufficient style differences, such as turning right, going forward, turning left, etc. All the above predictions prove the effectiveness of the proposed multi-style prediction strategy qualitatively.

#### V. CONCLUSION

Forecasting agents' possible future trajectories in crowd spaces is still challenging due to agents' uncertain personalized

future choices and the changeable video context. Although many researchers are committed to this task by modeling agents' stochastic interactive behaviors via generative neural networks, or their various intention or destination distributions in the goal-driven approaches, most of them model all kinds of agents' behaviors into a "single" feature distribution. It means that they are always challenging to give diversified future predictions with different-enough behavior styles for agents with diverse preferences and personalizations. In this manuscript, we tackle this problem by introducing a novel multi-style prediction strategy, therefore trying to give multiple future predictions with sufficient style differences. We propose the MSN, a transformer-based multi-style trajectory prediction network to predict agents' trajectories in a multi-style way. We adaptively divide agents' behaviors into different categories through their interactive context and end-point plannings. Then, we employ and train a series of generators (or called the style channels) accordingly with the constraints of the novel stylization loss. In this way, different style channels may focus on different patterns of agents' behavior representations, thereby giving differentiated predictions with specific styles. Experiments demonstrate that both MSN outperforms most of the current state-of-the-art prediction models, and can be adapted to various complex prediction scenarios. The visualized qualitative experimental results also show the effectiveness of the multi-style prediction strategy. The proposed models could provide diversified future choices with sufficient differences that meet the interactive constraints. In the future, we will continue to explore a suitable way to give differentiated and categorized future predictions for multiple kinds of agent, and try to address the existing failed prediction cases.

## APPENDIX A TRANSFORMER DETAILS

We employ the Transformer [51] as the backbone to encode trajectories and the scene context in each of the two subnetworks. Several trajectory prediction methods (like [34], [35]) have already tried to employ Transformers as their backbones. Experimental results have shown excellent improvements. Transformers can be regarded as a kind of sequence-tosequence (seq2seq) model [51]. Unlike other recurrent neural networks, the critical idea of Transformers is to use attention layers instead of the recurrent cells. With the multi-head selfattention layers [51], the long-distance items in the sequence could directly affect each other without passing through many recurrent steps or convolutional layers. In other words, Transformers can better learn the long-distance dependencies in the sequence while reducing the additional overhead caused by the recurrent calculation. The Transformer we used in the proposed MSN has two main parts, the Transformer Encoder and the Transformer Decoder. Both these two components are made up of several attention layers.

## A. Attention Layers

Following definitions in [51], each layer's multi-head dot product attention with H heads is calculated as:

$$\begin{split} & \text{Attention}(q,k,v) = \text{softmax}\left(\frac{qk^T}{\sqrt{d}}\right)v, \\ & \text{MultiHead}(q,k,v) = \text{fc}\left(\text{concat}(\{\text{Attention}_i(q,k,v)\}_{i=1}^H)\right). \end{split}$$

In the above equation, fc() denotes one fully connected layer that concatenates all heads' outputs. Query matrix q, key matrix k, and value matrix v, are the three inputs. Each attention layer also contains an MLP (denoted as  $MLP_a$ ) to extract the attention features further. It contains two fully connected layers. ReLU activations are applied in the first layer. Formally,

$$f_o = ATT(q, k, v) = MLP_a(MultiHead(q, k, v)),$$
 (20)

where q, k, v are the attention layer's inputs, and  $f_o$  represents the layer output.

#### B. Transformer Encoder

The transformer encoder comprises several encoder layers, and each encoder layer contains an attention layer and an encoder MLP (MLP<sub>e</sub>). Residual connections and normalization layers are applied to prevent the network from overfitting. Let  $h^{(l+1)}$  denote the output of l-th encoder layer, and  $h^{(0)}$  denote the encoder's initial input. For l-th encoder layer, we have

$$a^{(l)} = ATT(h^{(l)}, h^{(l)}, h^{(l)}) + h^{(l)},$$

$$a_n^{(l)} = Normalization(a^{(l)}),$$

$$c^{(l)} = MLP_e(a_n^{(l)}) + a_n^{(l)},$$

$$h^{(l+1)} = Normalization(c^{(l)}).$$
(21)

#### C. Transformer Decoder

Like the Transformer encoder, the Transformer decoder comprises several decoder layers, and each is stacked with two different attention layers. The first attention layer focuses on the essential parts in the encoder's outputs  $h_e$  queried by the decoder's input X. The second is the same self-attention layer as in the encoder. Similar to Equation 21, we have:

$$a^{(l)} = ATT(h^{(l)}, h^{(l)}, h^{(l)}) + h^{(l)},$$

$$a_n^{(l)} = Normalization(a^{(l)}),$$

$$a_2^{(l)} = ATT(h_e, h^{(l)}, h^{(l)}) + h^{(l)},$$

$$a_{2n}^{(l)} = Normalization(a_2^{(l)})$$

$$c^{(l)} = MLP_d(a_{2n}^{(l)}) + a_{2n}^{(l)},$$

$$h^{(l+1)} = Normalization(c^{(l)}).$$
(22)

## D. Positional Encoding

Before inputting agents' representations or trajectories into the Transformer, we add the positional coding to inform

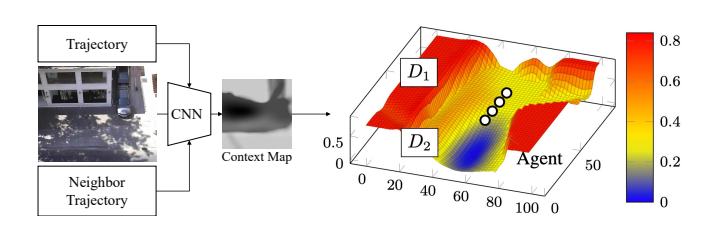


Fig. 10. Visualization of someone's context map. A lower semantic label (colored in blue) means that the place has a higher possibility for that agent to move towards, while a higher label (colored in red) means lower possibility.

each timestep's relative position in the sequence. The position coding  $f_e^t$  at step t  $(1 \le t \le t_h)$  is obtained by:

$$f_e^t = \left( f_{e0}^t, ..., f_{ei}^t, ..., f_{ed-1}^t \right) \in \mathbb{R}^d,$$
where  $f_{ei}^t = \begin{cases} \sin\left(t/10000^{d/i}\right), & i \text{ is even;} \\ \cos\left(t/10000^{d/(i-1)}\right), & i \text{ is odd.} \end{cases}$  (23)

Then, we have the positional coding matrix  $f_e$  that describes  $t_h$  steps of sequences:

$$f_e = (f_e^1, f_e^2, ..., f_e^{t_h})^T \in \mathbb{R}^{t_h \times d}.$$
 (24)

The final Transformer input  $X_T$  is the addition of the original input X and the positional coding matrix  $f_e$ . Formally,

$$X_T = X + f_e \in \mathbb{R}^{t_h \times d}. \tag{25}$$

## E. Transformer Details

We employ L=4 layers of encoder-decoder structure with H=8 attention heads in each Transformer-based subnetworks. The  $\mathrm{MLP}_e$  and the  $\mathrm{MLP}_d$  have the same shape. Both of them consist of two fully connected layers. The first layer has 512 output units with the ReLU activation, and the second layer has 128 but does not use any activations. The output dimensions of fully connected layers used in multihead attention layers are set to d=128.

## APPENDIX B INTERACTION REPRESENTATION

In the proposed MSN, we use the context map [45] to describe agents' interaction details through a two-dimensional energy map, which is inferred from scene images and their neighbors' trajectories. Considering both social and scene interactions, it provides potential attraction or repulsion areas for the target agent. Although the focus of this manuscript is not on the modeling of interactive behaviors, we still show the effect of this part, for it is a crucial research part of the trajectory prediction task. We visualize one agent's context map in zara1 dataset in Fig. 10. The target moves from about  $(x_0, y_0) = (50, 80)$  to the current (x, y) = (50, 50) during observation period.

• Scene constraints: The scene's physical constraints indicate where they could not move. The context map gives a higher enough value ( $\approx 1$ ) to show these areas. For example, the higher semantic label in the area  $D_1 = \{(x,y)|x \leq 20\}$  reminds pedestrians not to enter the road

- at the bottom of the zara1 scene. Similarly, another high-value area  $\{(x,y)|x\geq 80,y\leq 50\}$  reminds pedestrians not to enter the ZARA shop building except the door. It illustrates the ability of the context map to model the scene's physical constraints.
- Social interaction: Social interaction refers to the interactive behaviors among agents, such as avoiding and following. The context map does not describe the interaction behavior directly but provides lower semantic labels to areas conducive to agents' passage and higher semantic labels that are not. For example, the high-value area D2 = {(x,y)|20 ≤ x ≤ 40, y ≤ 80} shows another group of agents' possible walking place in the future who walk towards the target. The target agent will naturally avoid this area when planning his future activities. Context maps follow the lowest semantic label strategy to describe agents' behaviors. A place with a lower semantic label means that the target agent is more likely to pass through. Thus, it could show agents' social behaviors in the 2D map directly.

#### REFERENCES

- R. Mehran, A. Oyama, and M. Shah, "Abnormal crowd behavior detection using social force model," in 2009 IEEE Conference on Computer Vision and Pattern Recognition. IEEE, 2009, pp. 935–942.
- [2] H. Ergezer and K. Leblebicioğlu, "Anomaly detection and activity perception using covariance descriptor for trajectories," in *European Conference on Computer Vision*. Springer, 2016, pp. 728–742.
- [3] S. Pellegrini, A. Ess, K. Schindler, and L. Van Gool, "You'll never walk alone: Modeling social behavior for multi-target tracking," in 2009 IEEE 12th International Conference on Computer Vision. IEEE, 2009, pp. 261–268.
- [4] F. Saleh, S. Aliakbarian, M. Salzmann, and S. Gould, "Artist: Autoregressive trajectory inpainting and scoring for tracking," arXiv preprint arXiv:2004.07482, 2020.
- [5] P. Trautman and A. Krause, "Unfreezing the robot: Navigation in dense, interacting crowds," in 2010 IEEE/RSJ International Conference on Intelligent Robots and Systems. IEEE, 2010, pp. 797–803.
- [6] N. Deo and M. M. Trivedi, "Convolutional social pooling for vehicle trajectory prediction," in *Proceedings of the IEEE Conference on Com*puter Vision and Pattern Recognition Workshops, 2018, pp. 1468–1476.
- [7] N. Deo, A. Rangesh, and M. M. Trivedi, "How would surround vehicles move? a unified framework for maneuver classification and motion prediction," *IEEE Transactions on Intelligent Vehicles*, vol. 3, no. 2, pp. 129–140, 2018.
- [8] H. Cui, V. Radosavljevic, F.-C. Chou, T.-H. Lin, T. Nguyen, T.-K. Huang, J. Schneider, and N. Djuric, "Multimodal trajectory predictions for autonomous driving using deep convolutional networks," in 2019 International Conference on Robotics and Automation (ICRA). IEEE, 2019, pp. 2090–2096.
- [9] Y. Li, L. Xin, D. Yu, P. Dai, J. Wang, and S. E. Li, "Pedestrian trajectory prediction with learning-based approaches: A comparative study," in 2019 IEEE Intelligent Vehicles Symposium (IV). IEEE, 2019, pp. 919– 926
- [10] A. Alahi, V. Ramanathan, K. Goel, A. Robicquet, A. A. Sadeghian, L. Fei-Fei, and S. Savarese, "Learning to predict human behavior in crowded scenes," in *Group and Crowd Behavior for Computer Vision*. Elsevier, 2017, pp. 183–207.
- [11] Y. Chai, B. Sapp, M. Bansal, and D. Anguelov, "Multipath: Multiple probabilistic anchor trajectory hypotheses for behavior prediction," arXiv preprint arXiv:1910.05449, 2019.
- [12] T. Phan-Minh, E. C. Grigore, F. A. Boulton, O. Beijbom, and E. M. Wolff, "Covernet: Multimodal behavior prediction using trajectory sets," in *Proceedings of the IEEE/CVF Conference on Computer Vision and Pattern Recognition*, 2020, pp. 14074–14083.
- [13] A. Alahi, K. Goel, V. Ramanathan, A. Robicquet, L. Fei-Fei, and S. Savarese, "Social lstm: Human trajectory prediction in crowded spaces," in *Proceedings of the IEEE conference on computer vision and* pattern recognition, 2016, pp. 961–971.

- [14] A. Gupta, J. Johnson, L. Fei-Fei, S. Savarese, and A. Alahi, "Social gan: Socially acceptable trajectories with generative adversarial networks," in Proceedings of the IEEE Conference on Computer Vision and Pattern Recognition, 2018, pp. 2255–2264.
- [15] A. Sadeghian, V. Kosaraju, A. Sadeghian, N. Hirose, H. Rezatofighi, and S. Savarese, "Sophie: An attentive gan for predicting paths compliant to social and physical constraints," in *Proceedings of the IEEE Conference* on Computer Vision and Pattern Recognition, 2019, pp. 1349–1358.
- [16] V. Kosaraju, A. Sadeghian, R. Martín-Martín, I. Reid, H. Rezatofighi, and S. Savarese, "Social-bigat: Multimodal trajectory forecasting using bicycle-gan and graph attention networks," in *Advances in Neural Information Processing Systems*, 2019, pp. 137–146.
- [17] B. Ivanovic and M. Pavone, "The trajectron: Probabilistic multi-agent trajectory modeling with dynamic spatiotemporal graphs," in *Proceedings of the IEEE International Conference on Computer Vision*, 2019, pp. 2375–2384.
- [18] P. Kothari, S. Kreiss, and A. Alahi, "Human trajectory forecasting in crowds: A deep learning perspective," arXiv preprint arXiv:2007.03639, 2020
- [19] K. Mangalam, H. Girase, S. Agarwal, K.-H. Lee, E. Adeli, J. Malik, and A. Gaidon, "It is not the journey but the destination: Endpoint conditioned trajectory prediction," in *European Conference on Computer Vision*, 2020, pp. 759–776.
- [20] H. Tran, V. Le, and T. Tran, "Goal-driven long-term trajectory prediction," in *Proceedings of the IEEE/CVF Winter Conference on Applications of Computer Vision*, 2021, pp. 796–805.
- [21] A. Rudenko, L. Palmieri, M. Herman, K. M. Kitani, D. M. Gavrila, and K. O. Arras, "Human motion trajectory prediction: A survey," *The International Journal of Robotics Research*, vol. 39, no. 8, pp. 895–935, 2020.
- [22] A. Vemula, K. Muelling, and J. Oh, "Social attention: Modeling attention in human crowds," in 2018 IEEE international Conference on Robotics and Automation (ICRA). IEEE, 2018, pp. 1–7.
- [23] Y. Xu, Z. Piao, and S. Gao, "Encoding crowd interaction with deep neural network for pedestrian trajectory prediction," in *Proceedings of* the IEEE Conference on Computer Vision and Pattern Recognition, 2018, pp. 5275–5284.
- [24] P. Zhang, W. Ouyang, P. Zhang, J. Xue, and N. Zheng, "Sr-Istm: State refinement for lstm towards pedestrian trajectory prediction," in Proceedings of the IEEE Conference on Computer Vision and Pattern Recognition, 2019, pp. 12085–12094.
- [25] P. Zhang, J. Xue, P. Zhang, N. Zheng, and W. Ouyang, "Social-aware pedestrian trajectory prediction via states refinement lstm," *IEEE transactions on pattern analysis and machine intelligence*, 2020.
- [26] H. Xue, D. Q. Huynh, and M. Reynolds, "Ss-Istm: A hierarchical lstm model for pedestrian trajectory prediction," in 2018 IEEE Winter Conference on Applications of Computer Vision (WACV). IEEE, 2018, pp. 1186–1194.
- [27] M. Lisotto, P. Coscia, and L. Ballan, "Social and scene-aware trajectory prediction in crowded spaces," in *Proceedings of the IEEE International* Conference on Computer Vision Workshops, 2019, pp. 0–0.
- [28] H. Manh and G. Alaghband, "Scene-Istm: A model for human trajectory prediction," arXiv preprint arXiv:1808.04018, 2018.
- [29] J. Liang, L. Jiang, J. C. Niebles, A. G. Hauptmann, and L. Fei-Fei, "Peeking into the future: Predicting future person activities and locations in videos," in *Proceedings of the IEEE Conference on Computer Vision and Pattern Recognition*, 2019, pp. 5725–5734.
- [30] R. Liang, Y. Li, X. Li, J. Zhou, W. Zou et al., "Temporal pyramid network for pedestrian trajectory prediction with multi-supervision," arXiv preprint arXiv:2012.01884, 2020.
- [31] J. Liang, L. Jiang, and A. Hauptmann, "Simaug: Learning robust representations from simulation for trajectory prediction," in *Proceedings of the European conference on computer vision (ECCV)*, August 2020.
- [32] Y. Huang, H. Bi, Z. Li, T. Mao, and Z. Wang, "Stgat: Modeling spatial-temporal interactions for human trajectory prediction," in *Proceedings of the IEEE International Conference on Computer Vision*, 2019, pp. 6272–6281.
- [33] A. Mohamed, K. Qian, M. Elhoseiny, and C. Claudel, "Social-stgcnn: A social spatio-temporal graph convolutional neural network for human trajectory prediction," in *Proceedings of the IEEE/CVF Conference on Computer Vision and Pattern Recognition*, 2020, pp. 14424–14432.
- [34] C. Yu, X. Ma, J. Ren, H. Zhao, and S. Yi, "Spatio-temporal graph transformer networks for pedestrian trajectory prediction," in *European Conference on Computer Vision*. Springer, 2020, pp. 507–523.
- [35] F. Giuliari, I. Hasan, M. Cristani, and F. Galasso, "Transformer networks for trajectory forecasting," pp. 10335–10342, 2021.

- [36] P. Kothari, B. Sifringer, and A. Alahi, "Interpretable social anchors for human trajectory forecasting in crowds," in *Proceedings of the IEEE/CVF Conference on Computer Vision and Pattern Recognition*, 2021, pp. 15556–15566.
- [37] N. Lee, W. Choi, P. Vernaza, C. B. Choy, P. H. Torr, and M. Chandraker, "Desire: Distant future prediction in dynamic scenes with interacting agents," in *Proceedings of the IEEE Conference on Computer Vision* and Pattern Recognition, 2017, pp. 336–345.
- [38] J. Amirian, J.-B. Hayet, and J. Pettré, "Social ways: Learning multi-modal distributions of pedestrian trajectories with gans," in *Proceedings of the IEEE Conference on Computer Vision and Pattern Recognition Workshops*, 2019, pp. 0–0.
- [39] K. Mangalam, Y. An, H. Girase, and J. Malik, "From goals, waypoints & paths to long term human trajectory forecasting," arXiv preprint arXiv:2012.01526, 2020.
- [40] E. Rehder and H. Kloeden, "Goal-directed pedestrian prediction," in Proceedings of the IEEE International Conference on Computer Vision Workshops, 2015, pp. 50–58.
- [41] E. Rehder, F. Wirth, M. Lauer, and C. Stiller, "Pedestrian prediction by planning using deep neural networks," in 2018 IEEE International Conference on Robotics and Automation (ICRA). IEEE, 2018, pp. 5903–5908.
- [42] N. Rhinehart, R. McAllister, K. Kitani, and S. Levine, "Precog: Prediction conditioned on goals in visual multi-agent settings," in *Proceedings of the IEEE International Conference on Computer Vision*, 2019, pp. 2821–2830.
- [43] N. Rhinehart, K. M. Kitani, and P. Vernaza, "R2p2: A reparameterized pushforward policy for diverse, precise generative path forecasting," in Proceedings of the European Conference on Computer Vision (ECCV), 2018, pp. 772–788.
- [44] R. Quan, L. Zhu, Y. Wu, and Y. Yang, "Holistic 1stm for pedestrian trajectory prediction," *IEEE transactions on image processing*, vol. 30, pp. 3229–3239, 2021.
- [45] B. Xia, C. Wong, Q. Peng, W. Yuan, and X. You, "Cscnet: Contextual semantic consistency network for trajectory prediction in crowded spaces," 2021.
- [46] T. Salzmann, B. Ivanovic, P. Chakravarty, and M. Pavone, "Trajectron++: Dynamically-feasible trajectory forecasting with heterogeneous data," in Computer Vision–ECCV 2020: 16th European Conference, Glasgow, UK, August 23–28, 2020, Proceedings, Part XVIII 16. Springer, 2020, pp. 683–700.
- [47] B. Pang, T. Zhao, X. Xie, and Y. N. Wu, "Trajectory prediction with latent belief energy-based model," in *Proceedings of the IEEE/CVF Conference on Computer Vision and Pattern Recognition*, 2021, pp. 11814–11824.
- [48] J. Liang, L. Jiang, K. Murphy, T. Yu, and A. Hauptmann, "The garden of forking paths: Towards multi-future trajectory prediction," in *Proceedings of the IEEE/CVF Conference on Computer Vision and Pattern Recognition*, 2020, pp. 10508–10518.
- [49] A. Lerner, Y. Chrysanthou, and D. Lischinski, "Crowds by example," Computer Graphics Forum, vol. 26, no. 3, pp. 655–664, 2007.
- [50] A. Robicquet, A. Sadeghian, A. Alahi, and S. Savarese, "Learning social etiquette: Human trajectory understanding in crowded scenes," in *European conference on computer vision*. Springer, 2016, pp. 549– 565.
- [51] A. Vaswani, N. Shazeer, N. Parmar, J. Uszkoreit, L. Jones, A. N. Gomez, Ł. Kaiser, and I. Polosukhin, "Attention is all you need," in *Advances in neural information processing systems*, 2017, pp. 5998–6008.